

Design and Modelling of a Cooling Unit by Adsorption Geothermal Heat Pump in a Tropical Climate Zones

ABSTRACT

This work is a contribution of a modelling of air conditioner by adsorption for a habitat in a tropical climate. The system mainly consists of a captor adsorber powered by a geothermal heat pump (HP), a condenser and an evaporator. We use the zeolite/methanol couple and the different thresholds temperatures to define the thermodynamic system cycle. Moreover, we use a methodology based on nodal approach to establish a heat and mass transfer equations. Dubinin-Astakhov thermodynamic model is employed to express the mass adsorbed, the coefficient of performance (COP) and the cold production. We make use of the climatic data in Comoros for 2009-2019 period to obtain the ambient temperature. The model validation is done by comparing the shape of the cycle we obtain with the state of the art. First, the results show a relationship between temperature, pressure and adsorbed mass. The increase in temperature is accompanied by an increase of pressure and a decrease of adsorbed mass, and in the same way a decrease in the temperature causes a decrease in the pressure as well as a decrease of adsorbed mass. The mixture zeolite/methanol reaches 356K at the regeneration temperature with an input water temperature of 363K. We observed the influence of main important parameters on the mixture temperature such as fluid input temperature, fluid velocity or zeolite thermal conductivity. Finally, we show the thresholds temperatures influence on the COP and

Keywords: Modelling, Adsorption, Zeolite, Air conditioning, Comoros

NOMENCLATURE

Mains letters

C_p	Specific heat (J/kg/K)
E_a	Activation energy (J)
e_p	Thickness (m)
DF	Density flux (W/m ²)
h	Transfer coefficient (W/m ² .K)
L	Latent heat (J/kg)
L_c	Length (m)
M	Mass (kg)
m	Adsorbate concentration (kg/kg)
n	Dubinin-Astakhov constant
P	Pressure (Pa)
P_s	Saturation pressure (Pa)
Q_{des}	Desorption heat (J)
Q_{ev}	Cold production (J)
Q_T	Heat provides adsorber (J)
R	Gas characteristic constant
S	Surface (m ²)
T	Temperature (K)
t	Time (s)

Exponents

ads	Adsorption
cv	Convection
des	Desorption
r	Radiative
x	Transfer mode

Index

amb	Ambient
cw	External wall
cd	Condenser
cond	Condensation
e	Methanol
ev	Evaporator
eva	Evaporation
f	Fluid
g	Regeneration
m	Mixture zeolite/methanol
me	Metal parts
p	Internal wall
sky	Sky

U	Velocity (m/s)	<i>soil</i>	Soil
w	Adsorption capacity (m^3)	$w1$	Internal face of Internal wall
ΔH	Isosteric heat (J/kg)	$w2$	External face of Internal wall
Δm	Mass cycled (kg/kg)	$w3$	Internal face of External wall
Greek letters		$w4$	External face of External wall
λ	Thermal conductivity (W/m/K)	z	zeolite
ρ	Density (kg/m^3)	-	-
Φ_i	Heat source (W/m^2)	-	-

1. INTRODUCTION

Building sector represents 40% of global total consumption [1], of which a large part concerns heating, ventilation or air conditioning systems. Energy used for air conditioning continues to grow. In 2100, such an amount of energy is estimated to increase by 72% due to the development of modern architectures, the improvement of socioeconomic living conditions and the affordable price of air conditioning systems [2] [3]. Reducing this energy passes by the improvement of the energy efficiency of the building's envelope, the thermal renovation of buildings or the development of low energy consumption systems. Adsorption cooling heat pumps are thermodynamic devices capable of producing cooling effects [4], with a low energy or renewable source. For several decades, they are used in industrial installations or in buildings' air conditioning systems [5]. These machines are alternatives helping solving ecological and energy problems. Indeed, the technology of these machines is simple, maintenance is easy, and the materials used are recyclable [6]. In addition, those technologies use refrigerants like water, methanol and ammonia with adsorbent such as zeolite or activated carbon which have no effect on the environment. However, most works on these systems have shown the existence of the same physical and thermodynamic limits related to a significant heat loss on the adsorber bed [7], an efficiency problem due to the slowness of heat and mass transfers [8], or a problem of the system cycle that is intermittent [9]. Thus, to improve the performance of machines, first works on adsorption cooling heat pump are directly interested in researching a heat

recovery strategy on the adsorbed bed [10]. Numerous analyses [11] [12] of adsorption heat pump system using many adsorbers have shown that the more the number of adsorbers increases, the more the heat recovery is important despite the rises in terms of size, weight and price of the machine. The two adsorber systems consist of using two of them in intermittent and phase opposition. This solution eliminates the intermittent factor of the machine. WANG and al. [13] realized an experimental study on the heat recovery process. They showed that the COP of two and four adsorber beds improved from 38 to 25% respectively. Other recent studies [14] [15] showed that the use of directed mass transfer channels or structures with metal organics in the adsorber bed makes it possible to capitalize the heat and mass transfers.

Overall, many studies on these systems focus on improving adsorbent/adsorbate couple, cycle and optimization system. CRITOPH [16] studied thermodynamic cycles with different adsorption couples for a solar refrigerant machine. He reported that the activated carbon/methanol couple gives a high COP compared with other couples. For this, he used the Dubinin-Astakhov model to calculate the COP of the cycle, assuming constant the heat source and temperature. WANG and al. [17] designed an adsorption machine for air conditioning using the zeolite/water couple. They highlighted the possibility of using a two-design system compounded by an adsorber, an evaporator and a condenser each. Their system had a high temperature of nearly 450°C for the exhaust gas due to combustion in a locomotive. WANG and ZHANG [18] showed that the use of multi-cooling tubes

improves the pump operation cycle and reduces the machine size. A multi-cooling tube is a tube in which an adsorber, a condenser and an evaporator are all completely housed for small adsorption cooling unit. HAMID and IMAM [19] approached as well an optimization but focused on the detailed design of a sorption reactor. DEMIR [20] showed that the regeneration of the adsorber bed of a zeolite/water heat pump can be done using microwave heating.

In addition, other studies analyzed the influence of system parameters or proposed a new model of the adsorption heat pump. SOLMUS and al. [21] developed a model with a cylindrical adsorber using the silica gel/water couple. They studied the influence of parameters such as the materials proprieties, the geometric configurations of the adsorber or the operating parameters. Theirs results indicate that the increases of evaporation pressure and hot source temperature increase the refrigeration quantity product. The increases of condensation pressure and cool source temperature decrease the refrigeration quantity product. SWARD and al. [22] reviewed the different characteristics that impacts of the cycle performance system with temperature limits, cycle times or position of the valve at the inlet and outlet of the adsorber bed. An increase of 1.2% of the COP was observed compared to the classic cycle for a heat source of 393 K, a condensation temperature of 303 K, an evaporation temperature of 278 K and a zeolite/water couple as a generator. Further, much effort [23] has been devoted to developing heat pumps with advanced adsorption cycles using thermal waves or reduction of regeneration heat by examining the impact of particles variations.

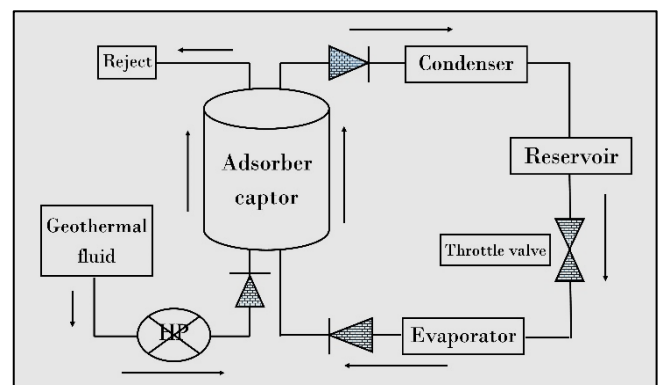
Comoros is an African country located in the Indian Ocean and has a tropical climate with a high temperature inside habitat. Currently, the country has a high potential of geothermal resource thanks to the presence of a rift associated with the active volcano Karthala with an 40MW estimated capacity [24]. These big reserves are still unexploited to this day. Its use attracts more and more experts in the energy sector along with those working in the

fields of economic and social development [25]. In addition, the country is currently experiencing an energy deficiency that is characterized by frequent electricity cut. Thus, the country's habitats rarely know a thermal comfort due to an insufficient energy. The main objective of this study is to contribute to the improvement of the thermal comfort of a habitat by an adsorption air conditioning system using geothermal heat pump. To do this, we propose a model of air conditioner by adsorption powered by a geothermal heat pump, using the zeolite/methanol couple. The system includes an adsorber captor, a condenser and an evaporator. First, we present a mathematical modeling of heat and mass transfer system. Then, we are making a numerical study of the system observing the temporal evolution of temperatures zeolite/methanol mixture, the pressure or the amounts of mass adsorbed. Finally, we evaluate the influence of the thresholds' parameters on the performance coefficient and amounts of cold production at evaporator.

2. MATERIALS AND METHODS

2.1. MODEL DESCRIPTION

The system consists mainly of an adsorber captor, a condenser, an evaporator. The adsorber captor, powered by a heat pump (HP), is a cylindrical tube composed by an internal small wall and an external big wall in which the geothermal fluid circulates. The captor length is equal to a 1.2m. The thicknesses of the internal and external captor walls are respectively equal to 0.1cm and 0.4cm. The zeolite layer, loaded with methanol, is deposited between the walls so that it occupies the entire volume available. The thickness of the mixture zeolite/methanol is equal to 2.9cm. The function of the heat pump is to inject a geothermal water inside the



captor.

Figure 1 shows the physical description of the system.

Figure 1: Schema of the system.

The cycle working principle is described perfectly by [4]. According to this study, the base cycle of the cooling unit is closed and intermittent. It breaks down into two phases: the regeneration-condensation and the adsorption-evaporation phases. The thermodynamic cycle is defined by the different thresholds temperatures of the system: evaporation temperature T_{eva} , condensation temperature T_{cond} , adsorption temperature T_{ads} and regeneration temperature T_g . The operation system begins when the geothermal fluid input at the adsorber. Flow rate and temperature to heat the metal parts of the adsorber are constant. The geothermal fluid is a hot water with a constant temperature equal to 363 K. In contact with the internal walls, it transmits the heat that propagates by convection. This heat is then transmitted by conduction to the zeolite/methanol mixture. The increase of the zeolite temperature creates the desorption of methanol vapor. The methanol vapor is redirected to the condenser and after crossing a throttle valve, the refrigerant passes to the evaporator and takes its heat at a definite pressure. We show all heat transfers on the captor adsorber in **Figure 2**.

2.2. MATHEMATICAL FORMULATION

2.2.1. SIMPLIFYING HYPOTHESES

The system is modeled according to the following assumptions:

- Conduction, convection and radiation transfers are unidirectional;
- Physical properties of materials are constant;
- Adsorber captor is cylindrical symmetrical;
- Entire mass adsorbed is condensed;
- Zeolite and methanol are similar to a homogeneous unit;
- The liquid condensate is easily removed under the effect of gravity;

- The methanol evaporates at constant pressure and condensates at constant pressure.

2.2.2. BASIC EQUATION

To establish the equations governing the transfers, we use a methodology based on nodal approach. The system is assimilated to a thermal system where each element is considered as an integral component of the system and corresponds to a single temperature.

The basic equation governing the evolution of the temperature of an element of the system over time is expressed by:

$$\frac{M_i \cdot Cp_i}{S_i} \left(\frac{\partial T_i}{\partial t} \right) = DF \times S_i + \sum_j h_{ij}^x \times (T_i - T_j) + (\phi_i)$$

2.2.3. HEAT AND MASS TRANSFERS EQUATIONS

The balance of heat and mass transfers of the cooling unit can be written as follow:

- For the geothermal fluid:

$$\begin{aligned} \frac{M_f \cdot Cp_f}{S_f} \left(\frac{\partial T_f}{\partial t} + U \frac{T_f - T_{f-1}}{L_c} \right) \\ = h_{f,w1}^{cv} (T_{w1} - T_f) \end{aligned}$$

- For the inner internal wall:

$$\begin{aligned} \frac{M_p \cdot Cp_p}{S_p} \left(\frac{\partial T_{w1}}{\partial t} \right) = h_{f,w1}^{cv} \cdot (T_f - T_{w1}) \\ + \frac{\lambda_p}{ep_p} (T_{w2} - T_{w1}) \end{aligned}$$

- For the outer internal wall:

$$\begin{aligned} \frac{M_p \cdot Cp_p}{S_p} \left(\frac{\partial T_{w2}}{\partial t} \right) = \frac{\lambda_p}{ep_p} (T_{w1} - T_{w2}) \\ + \frac{2\lambda_z}{ep_z} (T_m - T_{w2}) \end{aligned}$$

- For the mixture zeolite/methanol, the heat transfer is accompanied by a mass transfer.

When heating-desorption:

$$\begin{aligned}
& (M_z C p_z + m \cdot M_z C p_e) \left(\frac{\partial T_m}{\partial t} \right) \\
&= \delta \left[\Delta H_{des} M_z \frac{\partial m_e^{des}}{\partial t} \right. \\
&\quad \left. + M_z C p_e (T_m - T_{cd}) \frac{\partial m_e^{des}}{\partial t} \right] \\
&\quad + S_p \frac{2\lambda_z}{ep_z} (T_{w2} - T_m) \\
&\quad + S_{cw} \frac{2\lambda_z}{ep_z} (T_{w3} - T_m)
\end{aligned}$$

When cooling-adsorption:

$$\begin{aligned}
& (M_z C p_z + m \cdot M_z C p_e) \left(\frac{\partial T_m}{\partial t} \right) \\
&= \delta \left[\Delta H_{ads} M_z \frac{\partial m_e^{ads}}{\partial t} \right. \\
&\quad \left. - M_z C p_e (T_m - T_{ev}) \frac{\partial m_e^{ads}}{\partial t} \right] \\
&\quad + S_p \frac{2\lambda_z}{ep_z} (T_{w2} - T_m) \\
&\quad + S_{cw} \frac{2\lambda_z}{ep_z} (T_{w3} - T_m)
\end{aligned}$$

Where $\delta = 0$ for heating and cooling and $\delta = 1$, for desorption and adsorption.

- For the inner external wall:

$$\begin{aligned}
& \frac{M_{cw} \cdot C p_{cw}}{S_{cw}} \left(\frac{\partial T_{w3}}{\partial t} \right) \\
&= \frac{2\lambda_z}{ep_z} (T_m - T_{w3}) \\
&\quad + \frac{\lambda_{cw}}{ep_{cw}} (T_{w4} - T_{w3})
\end{aligned}$$

- For the outer external wall:

$$\begin{aligned}
& \frac{M_{cw} \cdot C p_{cw}}{S_{cw}} \left(\frac{\partial T_{w4}}{\partial t} \right) \\
&= \frac{\lambda_{cw}}{ep_{cw}} (T_{w3} - T_{w4}) \\
&\quad + h_{amb}^{cv} (T_{amb} - T_{w4}) \\
&\quad + h_{sky}^r (T_{sky} - T_{w4}) \\
&\quad + h_{soil}^r (T_{soil} - T_{w4})
\end{aligned}$$

- The heat transfer in the condenser is accompanied by a mass transfer. The condenser exchanges heat with ambient air by convection and with the sky and soil by radiation,

$$\begin{aligned}
& \frac{[M_{cd} C p_{cd} + m_e(t) C p_e] \frac{\partial T_{cd}}{\partial t}}{S_{cd}} \\
&= h_{amb}^{cv} (T_{amb} - T_{cd}) \\
&\quad + h_{sky}^r (T_{sky} - T_{cd}) \\
&\quad + h_{soil}^r (T_{soil} - T_{cd}) \\
&\quad + M_z S_{cd} \frac{\partial m_e^{des}}{\partial t} [L_{cd} (P_{cd}) \\
&\quad + C p_e (T_m - T_{cd})]
\end{aligned}$$

- The heat transfer in the evaporator is accompanied by a mass transfer,

$$\begin{aligned}
& \frac{[M_{ev} C p_{ev} + (m_e(t) - \Delta m \cdot m_z) C p_e] \frac{\partial T_{ev}}{\partial t}}{S_{ev}} \\
&= m_z S_{ev} \frac{\partial m_e^{ads}}{\partial t} [L_{ev} (P_{ev}) \\
&\quad - C p_e (T_m - T_{ev})]
\end{aligned}$$

2.2.4. THERMODYNAMIC MODEL

We use the Dubinin-Astakhov thermodynamic model and the equation expressing the mass adsorbed m_e is given by the following expression [4]:

$$m_e(t) = w_0 \rho_e(T) \exp \left\{ - \left(\frac{R}{E_a} \right)^n \left[T \ln \left(\frac{P_s(T)}{P} \right) \right]^n \right\}$$

For the saturation pressure, we express it with the Antoine formula by [26]:

$$P_s(T) = 133.33 \times \exp \left(18.5875 - \frac{3626.55}{T - 34.29} \right)$$

2.2.5. COEFFICIENT OF PERFORMANCE

The thermal coefficient of performance (COP) can be written with the following expression [27]:

$$COP = \frac{Q_{ev}}{Q_T}$$

The amount of cold produced at the evaporator is given by:

$$\begin{aligned}
Q_{ev} &= \Delta m \cdot m_z \left[L(T_{eva}) - \int_{T_{eva}}^{T_{cond}} C p_e(T) dT \right] \\
&= \Delta m \cdot m_z [L(T_{eva}) \\
&\quad - C p_e (T_{cond} - T_{eva})]
\end{aligned}$$

The amount of total heat required for the system to function can be expressed by:

$$Q_T = m_z \int_{T_a}^{T_g} C p_z dT + \left[m_z m_{max} \int_{T_a}^{T_{des}} C p_e(T) dT + m_z \int_{T_{des}}^{T_g} m(T) \cdot C p_e(T) dT \right] + \left(m_{me} \int_{T_a}^{T_g} C p_{me} dT \right) + Q_{des}$$

Where:

$$Q_{des} = \Delta m \cdot m_z \cdot \Delta H_{des}$$

2.3. RESOLUTION METHOD

Table 1 groups the input parameters used during the simulation. We used the implicit finite difference method to discretize the equations. Thus, we put the expressions we obtained in the following form:

$$C \frac{T(t + \Delta t) - T(t)}{\Delta t} = AT(t + \Delta t) + BD(t + \Delta t)$$

Where A, B, C and D are constants.

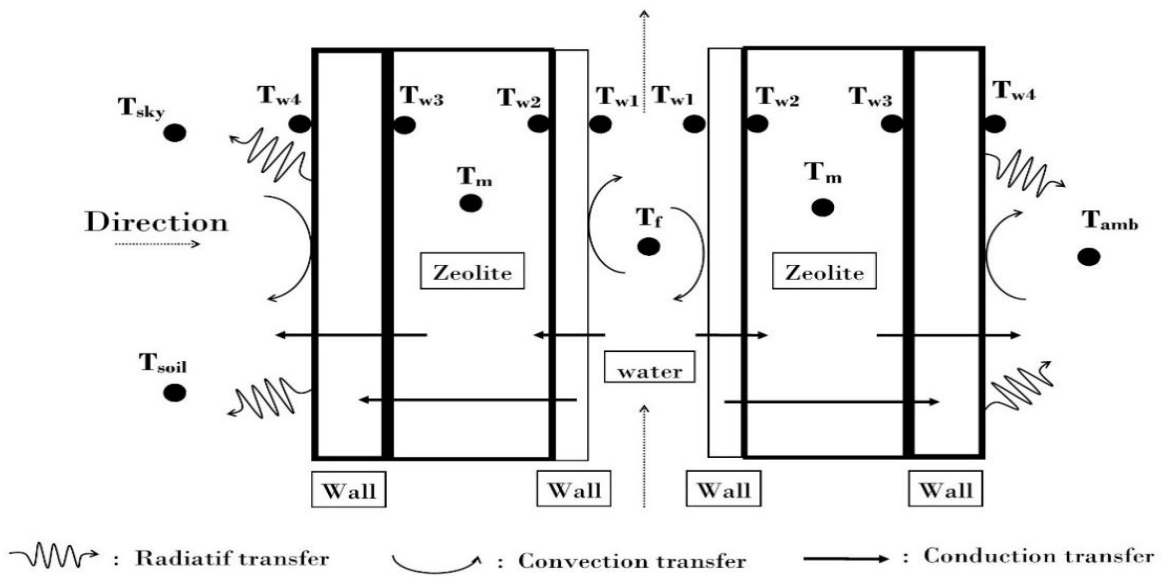


Figure 2: Schematic of adsorber captor heat transfers.

We used the Gauss algorithm to make the resolution by using an iterative calculation. It allows to determine the unknown variable at $(t + \Delta t)$ time in accordance with the function of the variable we know at the previous t with a criterion convergence.

The convergence was obtained when the following criterion was satisfied:

$$\frac{T^{t+\Delta t} - T^t}{T^{t+\Delta t}} \leq 10^{-3}$$

2.4. CLIMATIC DATA

We used the climatic data of typical November day in Comoros for 2009-2019 period. The ambient temperature is assimilated to sinusoidal functions. These days are marked by maximum and minimum average

temperatures respectively equal to 305.76K and 298.46K. **Figure 3** represents an ambient temperature.

3. RESULTS AND DISCUSSIONS

3.1. MODEL VALIDATION

In order to validate our model, we compared the shape of the cycle we obtained with the data G. C. Tubreoumya and al. [6] reported.

Figure 4 shows the evolution of the cycle of this study and the one G. C. Tubreoumya and al. obtained in their study of a refrigeration system by adsorption powered by a solar captor. They studied the zeolite/water couple. By comparing the two cycles, we found gaps in particular at the cooling and heating phases. These differences can be explained by the different simulation conditions, the simplifying

assumptions mentioned, and the numerical method we used for equations resolution or the physical parameters of the system components. In addition, the saturation pressure of their system is lower because they use water as refrigerant. This is normal because the vapor pressure of methanol is greater than that of water.

Figure 5 reports the validation of the condenser model. We observe that the condenser curve of our study follows normally the condenser curve Tubreoumya and al. [6] reported G. C. in their study. However, we

observe the same differences in particular when the condenser cools down. These differences can be explained by the different simulation conditions, the simplifying assumptions mentioned, and the numerical method used for resolution of equations or the physical parameters of the system components. The temperature of their condenser reaches its maximum at 320K while our condenser reaches its maximum at 323.9K at the end of the desorption phase.

The evaporator validation is showed in the **Figure 6**.

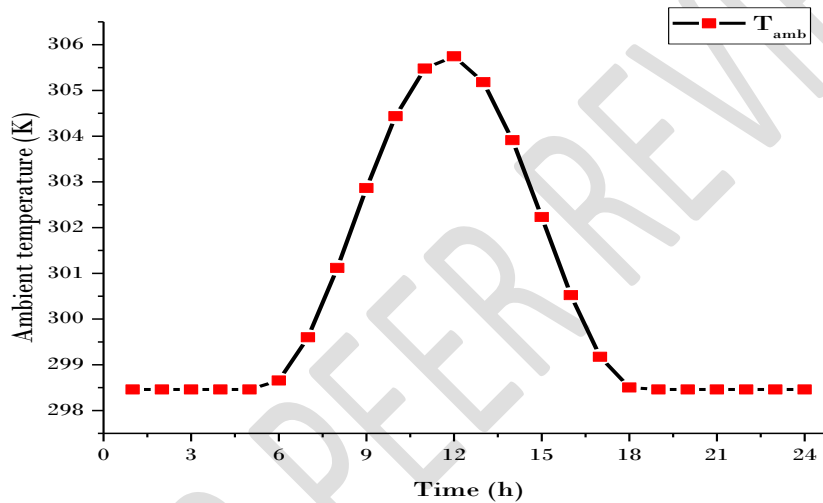


Figure 3: Ambient temperature for the typical day of November on 2009-2019 period.

By comparing the evaporator curve of our study with the evaporator curve G. C. Tubreoumya and al. [6] reported, we note that their trajectories are the same for most of the time. At the beginning of the evaporation phase, their evaporator temperature starts at 297K and reaches 275 K at the end of the evaporation phase while our evaporator starts at 298.45K and reaches 283K at the end of evaporation phase. These differences can be explained specifically by their study focusing on refrigeration machines while ours is about an air conditioning unit where it does not necessarily display a very low evaporator temperature.

3.2. THERMAL BEHAVIOR OF THE ADSORPTION COOLING UNIT

Temperature, pressure and adsorbed mass follow normally the evolution of the phases cycle and dictate its evolution. They are undeniably linked and we also show their curves in **Figure 7**. The increase of temperature is accompanied by an increase of pressure, and in the same way, a decrease of the temperature causes a decrease in pressure. The quantity of methanol vapor mass adsorbed from the zeolite bed according to the cycle phase is also represented on the **Figure 7**. In general, the look of the curves of

mass follows the evolution of the temperature of the cycle, and vice versa. The mixture zeolite/methanol begins with an adsorption temperature of 298.46K and 0.194kg/kg for maximum mass and reaches a 356.36K at regeneration temperature with 0.158kg/kg for minimum desorbed mass at end of desorption process under the condensation pressure. In fact, given the intermittent nature of these machines and several losses due to the system dimensioning parameters, the time between the phases are not necessarily equal compared to the cycle of the machine. This case explains for example a desorption time that lasts a little longer than adsorption time. Note that at the end of the adsorption-evaporation phase, the methanol vapor cannot be totally desorbed and the total mass of

adsorbed steam is less than the total mass of the initial steam at the end of the adsorption-evaporation.

Table1: Main input simulations parameters [4]

Symbol	Value	Symbol	Value
Cp_z	836J/kg/K	Cp_p	1 800J/kg/K
ρ_{cw}	1	w_o	0.269
	300kg/m ³		
T_f	363K	E_a	8134.10 ⁴ J
ρ_z	980kg/m ³	λ_z	2
ρ_p	1	λ_p	200.758Wm ⁻¹ K ⁻¹
	200kg/m ³		
P_{ev}	6 129Pa	Cp_{cw}	1278K/kg/K
P_{cd}	19 594Pa	n	2

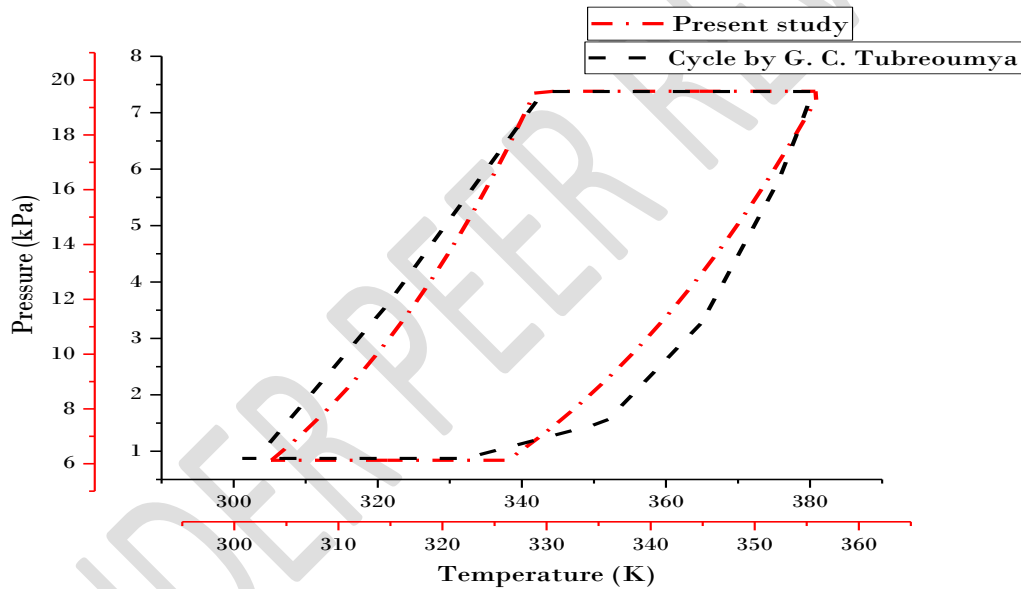


Figure 4: Cycle validation.



Figure 5: Condenser validation.

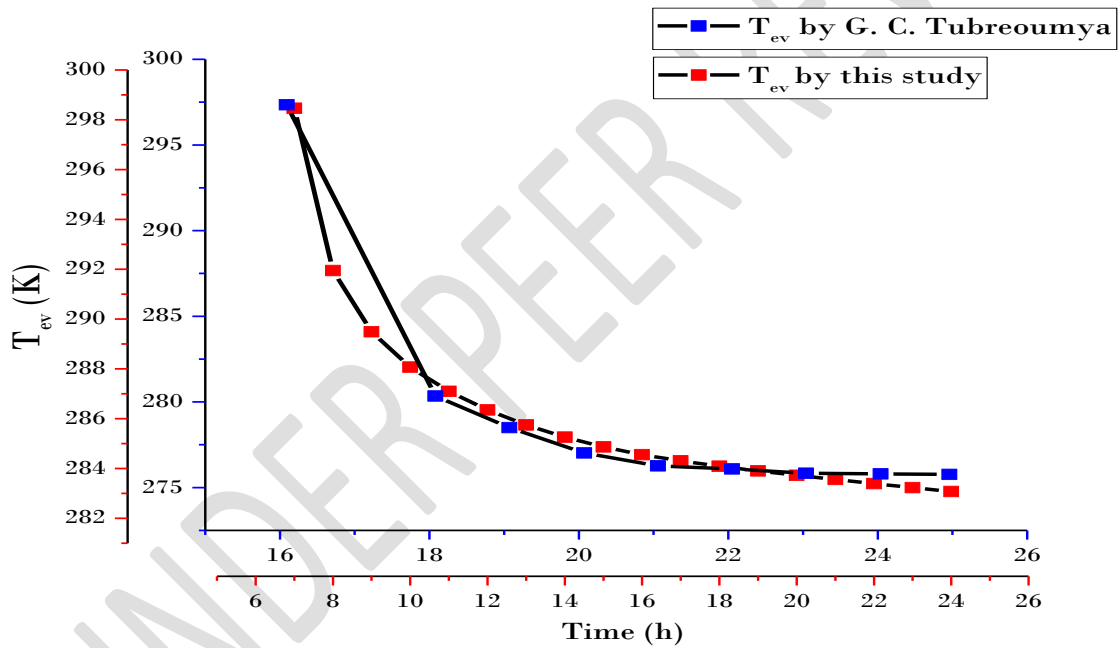


Figure 6: Evaporator validation.

3.3. INFLUENCE OF MAIN PARAMETERS ON THE MIXTURE TEMPERATURE

Figure 8 shows the influence of the geothermal fluid temperature at the input of the adsorber captor on the temperature of the mixture zeolite/methanol. An increase of the geothermal fluid temperature increases the mixture temperature on the adsorber and vice versa. For an input temperature of the

geothermal fluid of 333K, the mixture reaches a regeneration temperature of 329.28K. So, for an input temperature of 373 K, it reaches 365.31K of regeneration temperature. We explain this by the fact that the increase in fluid temperature increases the temperature of the internal wall by convection and the increase of the latter implies an increase of the zeolite temperature by conduction.

Figure 9 shows the influence of the fluid velocity input at the inlet of the captor on the temperature of the zeolite/methanol mixture. For this, we varied the geothermal fluid velocity from 0.01 to 0.09m/s. The results show that increasing the fluid velocity decreases the temperature of the zeolite especially at the heating-condensation phase. In fact, for a velocity of 0.01m/s, the zeolite can reach a maximum regeneration temperature equaling 359.08K. Whereas for a velocity of 0.09m/s, the zeolite reaches only 353.72

K. These tendencies are explained by the fact that the increase of the fluid geothermal velocity reduces the exchange coefficient between the fluid and internal wall. The reduction of this exchange coefficient implies a reduction in the heat flow between the geothermal fluid and the internal wall, which involves a less temperature at the zeolite. The influence of the geothermal fluid velocity is important on the heating-condensation phase. It is during the heating-condensation phase that the fluid velocity influences most the heating of the metal parts of the captor by the circulation of the hot fluid which is not the case during the cooling-adsorption phase.

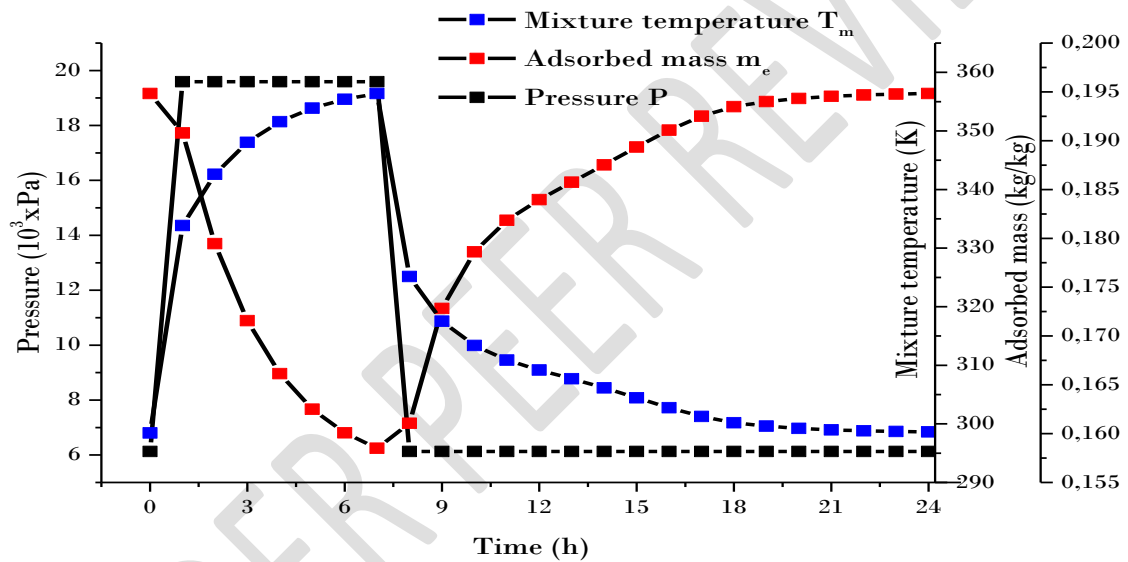


Figure 7: Evolution of the zeolite temperature, adsorbed mass and pressure.

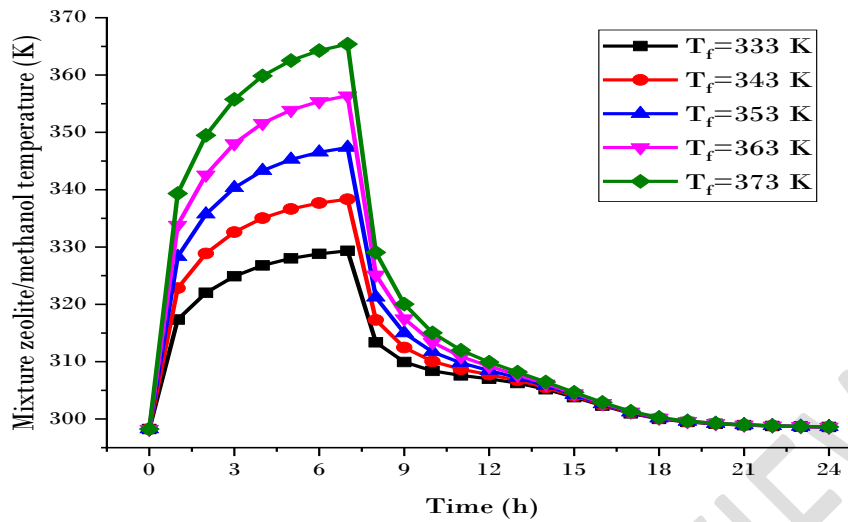


Figure 8: Influence of the input geothermal fluid temperature.

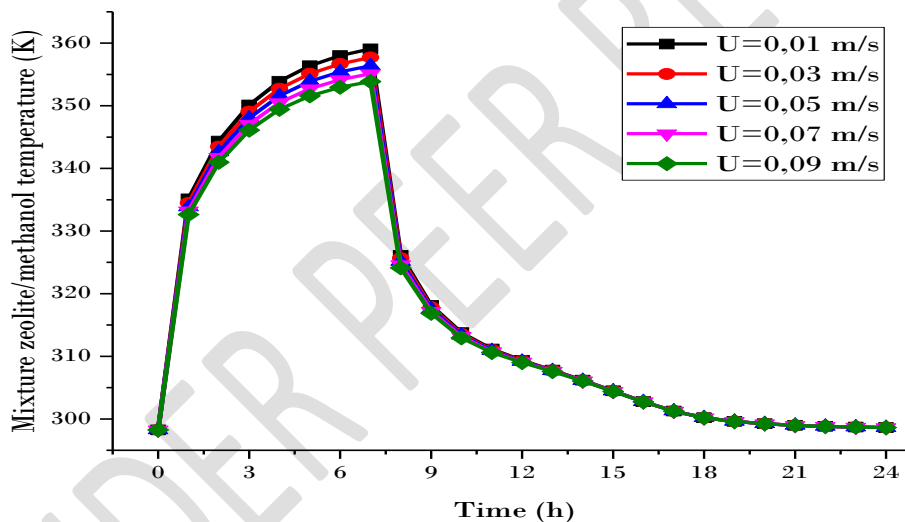


Figure 9: Influence of the fluid velocity.

During cooling-adsorption, the mixture is mostly cooled by the evaporation of methanol vapors in the evaporator and by the wall temperatures with the ambient air due to the cutoff of the fluid circulation.

Figure 10 shows the influence of the thermal conductivity of the zeolite on the temperature of zeolite/methanol mixture. Indeed, the increase of the zeolite conductivity implies an

increase in the temperature of the mixture. For a thermal conductivity of 2.8W/m.K . The mixture reaches a maximum regeneration temperature equaling 357.9K . For a thermal conductivity of 0.4W/m.K , it reaches a regeneration temperature equaling 337.72K . We explain these results by the fact that the increase in the thermal conductivity of the zeolite implies an increase in the exchanges between walls and zeolite.

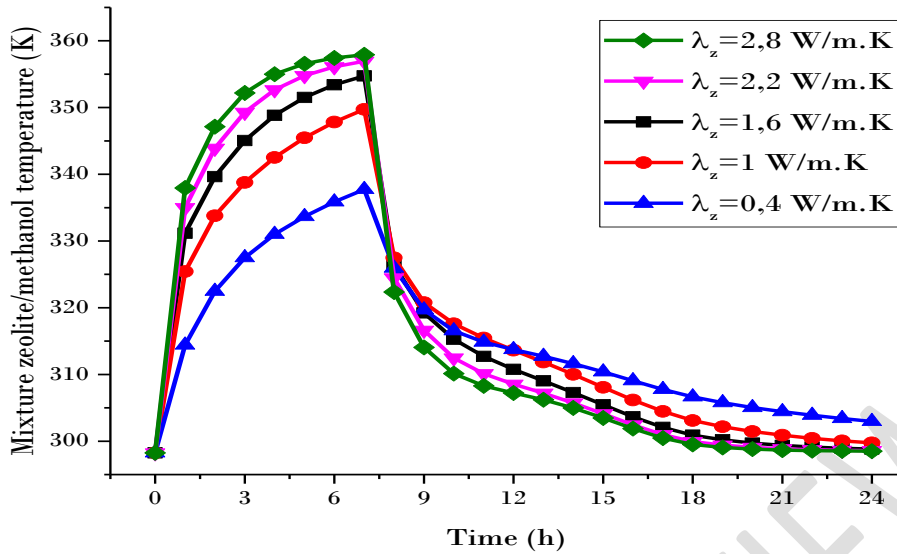


Figure 10: Influence of the zeolite thermal conductivity

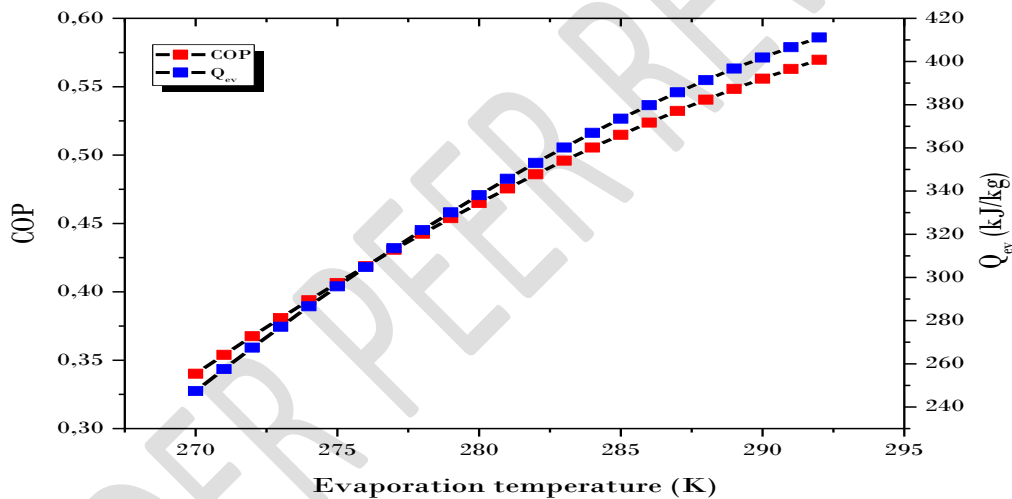


Figure 11: Influence of the evaporation temperature.

3.4. INFLUENCE OF THRESHOLDS TEMPERATURES ON PERFORMANCES

The following results are presented with thresholds temperatures for 280K as evaporation temperature, 298K as adsorption temperature, 301K as condensation temperature and 363K as regeneration temperature and they show that the system reaches 0.46 of COP and 338.078kJ/kg of cold product at evaporator. We look at the influence of these temperatures on the COP and the cold produced at the evaporator Q_{ev}

varying each time one of them and fixing the others as constant.

Figure 11 shows the influence of the evaporation temperature on the performances. We find that the increase of an evaporation temperature involves an increase of the COP as well as the amount of cold production. For an evaporation temperature from 270K to 292K, the system reaches respectively a COP that varies from 0.34 to 0.57 and a cold amount produced a value from 247.4 to 411.15kJ/kg. Indeed, the increase of the evaporation temperature rises the saturation pressure in the evaporator and the maximum amount of mass; this leads to an increase

cycle. An increase in the cycled mass implies a simultaneous increase in the amount of cold

produced at the evaporator and of the COP.

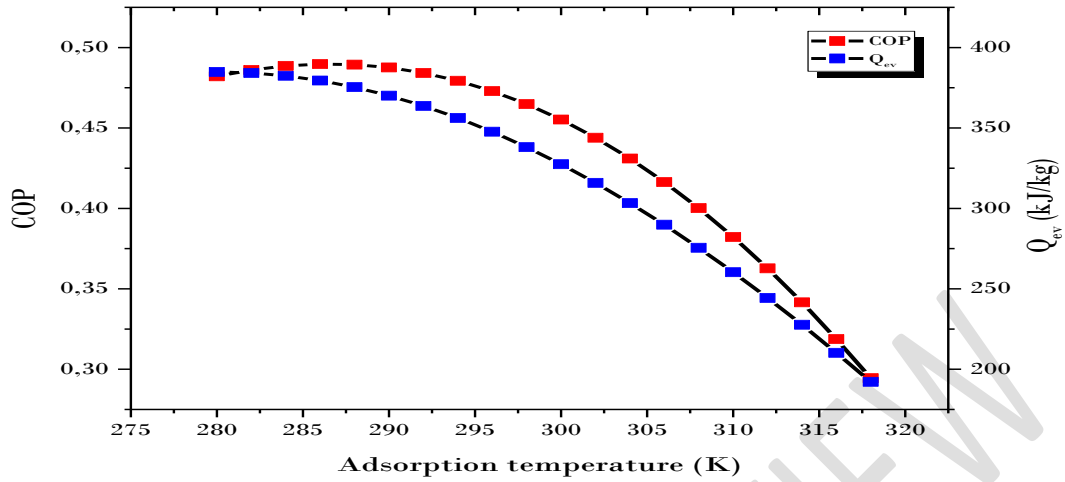


Figure 12: Influence of the adsorption temperature.

Figure 12 shows the influence of the adsorption temperature on the performances of the system. We have varied the adsorption temperature from 280 to 318K. It shows that the increase of the adsorption temperature decreases the COP and the amount of cold production. For this, we have respectively COP values varying from 0.482 to 0.294 and a cold quantity at the evaporator of a value varying from 384.83 to 192.15kJ/kg. Indeed, the increase in the adsorption temperature in the beginning of the cycle decreases the

maximum adsorbed mass, which consequently reduces the cycled mass and therefore the performance of the machine. However, a high decrease of the adsorption temperature can cause a reduction in the performance of the system as shown by the decline of the COP curve for a low enough temperature. It simply shows that a balance must be met at the beginning of the cycle and not start the cycle by a very low adsorption temperature. A very low temperature affects the balance of the relationship between the amount of cold production and the amount of useful heat.

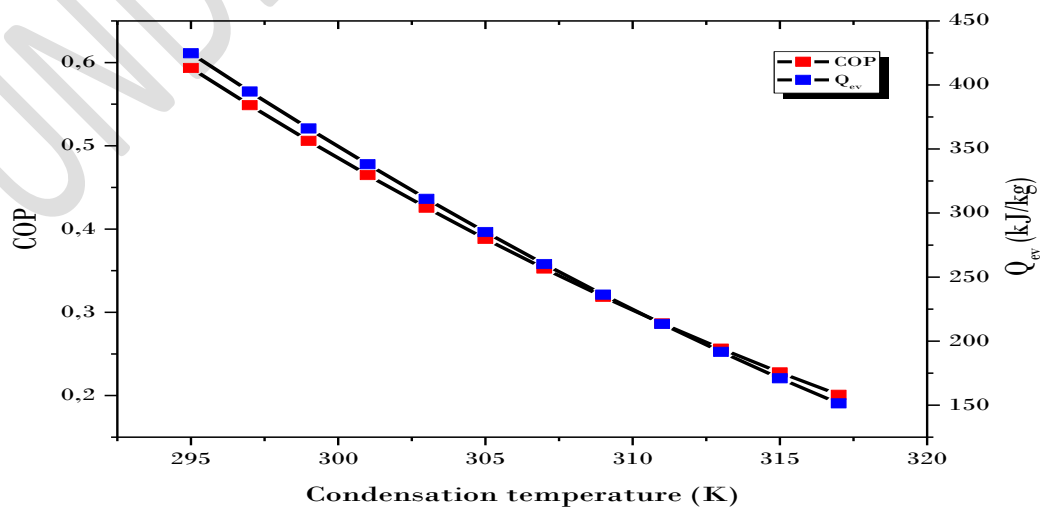


Figure 13: Influence of the condensation temperature.

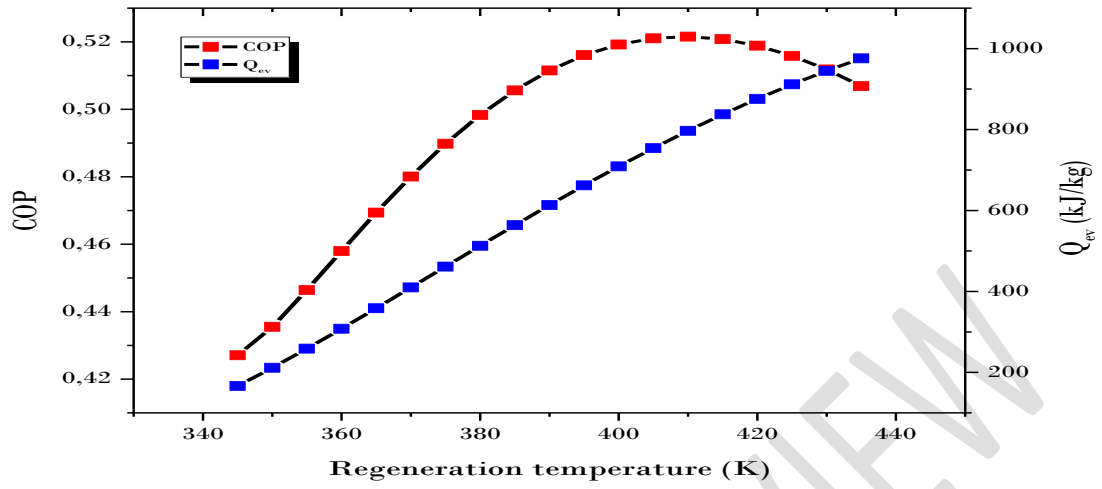


Figure 14: Influence of the regeneration temperature.

In **Figure 13**, we show the influence of the condensation temperature on the system performances. By varying the condensation temperature from 295 to 317K, we obtain a value from 0.593 to 0.2 for a COP and a quantity of cold production that varies from 424.7 to 151.34kJ/kg. Thus, it appears that the increase in the condensation temperature reduces the performance of the system. This is explained by the fact that the increase in the condensation temperature increases the saturation pressure to the condenser, hence an increase in the temperature of the desorption. However, the increase in desorption temperature decreases the amount of maximum mass and thus a decrease in the amount of cycled mass. This leads to the decrease in the COP and the amount of cold produced at the evaporator.

In **Figure 14**, we present the influence of the regeneration temperature on the cycle performance. For a regeneration temperature from 345 K to 435 K, we have a COP varying from 0.427 to 0.5 and a cold production from 166.41 to 975.9 kJ/kg. We observe that an increase in the regeneration temperature increases the performance of the system. Indeed, the increase in the regeneration temperature reduces the minimum mass and thus increases cycled mass, which leads to better performance at the system level. However, it is not necessary to increase infinitely regeneration temperatures because it also affects the physical properties of materials that are limited to transmit a high range of heat. In addition, the chemical and thermodynamic limits of adsorbent/adsorbate couples at high temperatures must be taken into account. That is why we observe that the COP reaches a maximum value although the amount of cold produced continues to increase.

4. CONCLUSION

We performed a contribution of a heat and mass transfers modelling of an air conditioning by adsorption. We used a geothermal fluid to heat a zeolite. The simulation results highlighted the bi-variant relationship between temperature, pressure and adsorbed mass. The mixture zeolite/methanol temperature is

the most important parameter and its evolution is directly related to the performances of the system. For an input fluid temperature of 363 K, the zeolite reached a regeneration temperature of 356.36 K. In addition, it appears that the increase of input fluid temperature or zeolite thermal conductivity increases the zeolite regeneration temperature. However, the increase of a fluid velocity decreases the zeolite regeneration temperature. In addition, an increase of the adsorption and condensation temperatures decrease the COP and the cold production at evaporator while an increase of the evaporation and regeneration temperatures increase the COP and cold production at evaporator. This cooling unit may be an alternative to the air conditioning system of buildings in Comoros using the geothermal resource that the country benefits from.

5. ACKNOWLEDGEMENTS

The Authors would like to thank the SCAC service of French Embassy to Comoros for the financial supports.

6.

7. REFERENCES

- [1] L. Pérez-Lombard, J. Ortiz and C. Pout, «A review on buildings energy consumption information, » *Energy and buildings*, 40(13), 394-398, 2008.
- [2] M. Isaac and v. Vuuren, D.P «Modeling global residential sector energy demand for heating and conditioning in the context of climate change, » *Energy Policy*, 37, 507-521, 2009.
- [3] Saha. B. B., Akisawa. A. and Kashiwagi T., «Solar/waste heat driven two-stage adsorption chiller: The prototype, » *Renewable Energy*, 23, 93-101, 2001.
- [4] D. El-Maktoume, X. Chesneau, Diallo A. and Randriamanantany Z. A, «Study of Habitat's Thermal Performance Equipped with an Adsorption Cooling Unit by Geothermal Heat Pump, » *Journal of Power and Energy Engineering*, 9, 26-52, 2021.
- [5] J. Y. Ausseur et J. P. Sauty, «L'exploitation des nappes francaises par pompes à chaleur: aspects hydrogéologiques, thermiques et législatifs, » *Hydrogeology in the Service of Man, Memoires of the 18th Congress of the International Association of Hydrogeologists*,

- 42-58, 1985.
- [6] G. C. Tubreoumya, A. O. Dissa, E. S. Tiendrebeogo, X. Chesneau, A. Compaoré, K. Haro, C. D. Konseibo, B. Zeghmati et J. Kouliadiati, «Contribution to the Modeling of a Solar Adsorption Refrigerator under the Climatic Conditions of Burkina Faso, » *Energy and Power Engineering*, 9, 119-135, 2017.
- [7] F. Meunier, «On the use of a zeolite 13X-H 20 intermittent cycle for the application to solar climatization of building, » *LS.E.S. Conference, Atlanta*, 739-743, 1979.
- [8] G. G. Ilis et H. Demir, «Influence of bed thickness and particle size on performance of microwave regenerated adsorption heat pump, » *International Journal of Heat and Mass Transfer*, 123, 16–24, 2018.
- [9] X. Li, X. Hou, X. Zhang et Z. Yuan, «A review on development of adsorption cooling—Novel beds and advanced cycles, » *Energy Convers. Manage.* 94, 221-232, 2015.
- [10] M. Pons et S. Szarzynski, «An adsorption cooling system with heat-regeneration: experimental and numerical study, » *Proceeding of the International Sorption Heat Pump Conference, Germany*, 625–30, 1999.
- [11] U. Wittstadt, G. Földner, E. Laurenz, A. Warlo, A. Große, R. Herrmann, L. Schnabel et W. Mittelbach, «A novel adsorption module with fiber heat exchangers: Performance analysis based on driving temperature differences, » *Renew. Energy*, 110, 154-161, 2017.
- [12] W. Zheng, W. Worek et G. Nowakowski, *International Journal of Energy Research* 20, pp. Performance of multi-bed sorption heat pump systems, 339–350, 1996.
- [13] X. Wang, H. T. Chua et K. C. Ng, «Experimental investigation of silica gel-water adsorption chillers with and without a passive heat recovery scheme, » *International Journal of Refrigeration*, 28(15), 756-65, 2005.
- [14] J. Ammann, B. Michel, A. Studart et P. Ruch, «Sorption rate enhancement in SAPO-34 zeolite by directed mass transfer channels, » *Int. J. Heat Mass Transf.* 130, 25-32, 2019.
- [15] R. Al-Dadah, S. Mahmoud, E. Elsayed, P. Youssef et F. Al-Mousawi, «Metal-organic framework materials for adsorption heat pumps, » *Energy* 190, ID:116356, 2020.
- [16] R. E. Critoph, «Performance limitations of adsorption cycles for solar cooling, » *Sol. Energy*, vol. 41(11), 21-31, 1988.
- [17] D. Wang, Z. Xia et J. Wu, «Design and performance prediction of a novel zeolite–water adsorption air conditioner, » *Energy Conversion and Management*, 47, 590–610, 2006.
- [18] D. Wang et J. Zhang, «Design and performance prediction of an adsorption heat pump with multi-cooling tubes, » *Energy Conversion and Management*, 50, 1157–1162, 2009.
- [19] H. Niazmand et I. Dabzadeh, «Numerical simulation of heat mass transfer in adsorbent beds with annular fins, » *International Journal of Refrigeration*, 35(13), 581-593, 2012.
- [20] H. Demir, «Development of microwave assisted zeolite-water adsorption heat pump, » *International Journal of refrigeration*, 36, 2289-2296, 2013.
- [21] I. Solmus, C. Yamali, C. Yıldırım et K. Bilen, «Transient behavior of a cylindrical adsorbent bed during the adsorption process, » *Applied Energy*, 142, 115–124, 2015.
- [22] B. K. Sward, M. D. LeVan et F. Meunier, «Adsorption heat pump modeling: the thermal wave process with local equilibrium, » *Applied Thermal Engineering*, 20, 759-780, 2000.
- [23] K. A. Ramzy, R. Kadoli et T. P. A. Babu, «Significance of axial heat conduction in non-isothermal adsorption process in a desiccant packed bed, » *International Journal of Thermal Sciences*, 76, 68-81, 2014.
- [24] I. Bogie et J. Charroy, «Comoros surface exploration, Geophysics and Summation,» *Jacobs, Auckland*, 2015.
- [25] G. G. Muchemi, S. A. Onacha et J. Wambugu, «Reconnaissance and Inception Report for Geothermal Resources Exploration Program of the Grande Comore,» *Internal KenGen Report for the Federal Government of Comoros*, Unpublished, 2008.
- [26] M. A. H. Ammar, B. Benhaoua et F. Bouras, «Thermodynamic analysis and performance of an adsorption refrigeration system driven by solar collector, » *Applied Thermal Engineering*, 112, 1289-1296, 2017.
- [27] A. Fadar, A. Mimet et M. Pérez-Garcia, «Modelling and performance study of a continuous adsorption refrigeration system driven by parabolic trough solar collector, » *Solar Energy*, 83, 850-861, 2009.